# Beam-foil spectroscopy of $n=3$ to $n=2$ transitions in highly stripped bismuth

D. D. Dietrich, A. Simionovici, M. H. Chen, G. Chandler,
C. J. Hailey, and P. O. Egan
*Lawrence Livermore National Laboratory, Livermore, California 94550*

P. H. Mokler and S. Reusch
*Gesellschaft für Schwerionenforschung (GSI), D-6100 Darmstadt, Federal Republic of Germany*

D. H. H. Hoffmann
*Max-Planck-Institute for Quantum Optics (MPQ), D-8046 Garching, Federal Republic of Germany*
(Received 10 October 1989)

The $n=3$ to 2 transitions in Ne-like, Na-like, and Mg-like bismuth were measured on the UNILAC accelerator at the Gesellschaft für Schwerionenforschung in Darmstadt, West Germany, using the Lawrence Livermore National Laboratory high-resolution double-crystal spectrometer. The measurements cover the region 10–14 keV with precisions of the order of 100 ppm and include electric-dipole and quadrupole transitions. Theoretical multiconfigurational Dirac-Fock calculations were made for the Ne-like system and compared to the experiment. The data exhibit energy shifts of 1.5–2.5 eV from the theory, confirming trends previously observed in tokamak experiments. The Na-like and Mg-like results are compared with unresolved transition array calculations.

## I. INTRODUCTION

The precision spectroscopy of highly charged heavy ions is a challenging field in atomic spectroscopy as it provides the testing ground for atomic-structure calculations. Knowledge of precise wavelengths for these systems is important in a number of related fields, from plasma diagnostics to astrophysics. The theory has to be compared to the experimental results to ascertain its validity in domains of strong fields and where many-body corrections are essential. The Ne-like system studied here tests the relativistic theory of multielectron atoms in strong Coulomb fields while also being sensitive to quantum electrodynamic (QED) corrections in multielectron systems.

The Ne-like system is particularly attractive for it features a closed $L$ shell and thus has relatively simple $n=3\rightarrow 2$ spectra. Ne-like ions are relatively easy to produce and are accessible for ions of considerably higher $Z$ than those with an open $K$ shell. Since the leading QED terms scale as $(Z\alpha)^4$ one can test the theory with lower experimental precision in this energy range. The major causes of disagreement between experiment and theory are the necessity to include Coster-Kronig fluctuations on the $2s$ states and QED effects for electrons with penetrating orbitals that probe the nucleus. This paper addresses the latter problem and reports on an experiment that improves the precision of our previous measurements[1] by more than a factor of 2.

## II. THEORY

At the present time, there exists no coherent and accurate solution to the relativistic many-electron problem. Instead, we rely on a calculational prescription, fragments of which are taken from quantum electrodynamic theory.[2] In the present work, the $n=3\rightarrow n=2$ transition energies of the $Bi^{73+}$ ion were calculated using the multiconfigurational Dirac-Fock method[3] (MCDF). The calculations include the effect of finite nuclear size and higher-order relativistic corrections: the transverse Breit interaction and QED corrections. The exchange of a virtual photon between two orbital electrons leads to a modification of the instantaneous Coulomb interaction. In our present calculations, the magnetic interaction and retardation corrections were taken into account through the use of the transverse Breit interaction in first-order perturbation theory.[4]

There are two main radiative corrections: self-energy and vacuum polarization. They arise from the interaction of the electrons with the radiation field. For heavy ions, one-electron self-energies are known only for the $1s$, $2s$, and $2p$ levels of the hydrogenic ions.[5] Self-energy corrections in the many-electron systems are not available except for the $K$ shell of heavy neutral atoms.[2] In the MCDF model,[3,4] the many-electron self-energy corrections are estimated by interpolating among Mohr's point Coulomb values[5] for the $1s$, $2s$, and $2p$ levels. A $n^{-3}$ scaling rule is used for the higher $n$ levels, coupled with an effective-charge screening approach to account for the screening effect due to the other electrons (MCDF-S). The vacuum polarization corrections are determined by evaluating the expectation value of the Uehling potential using Dirac-Fock wave functions. The $n=3\rightarrow n=2$ x-ray energies were also calculated using the hydrogenic self-energies (MCDF-H) instead of the phenomenological screened ones. The $2s$-$3p$ transition energies are lowered by $\sim 6$ eV when the hydrogenic self-energies are used.

The electron-electron correlation energies were taken into account approximately by using limited configuration interaction. It is assumed that the correlation

 

energies of the passive electrons from the ground and excited states cancel out. Separate calculations were performed for the ground and excited states. For the $1s^2 2s^2 2p^6$ ground state, the single configuration was used. For the upper $J=1$ odd states, coupled multiconfiguration calculations were carried out in the average-level scheme (MCDF-AL) using the configuration state functions (CSF's) from $2s^2 2p^5 3s$, $2s^2 2p^5 3d$, and $2s 2p^6 3p$ configurations. For the $J=2$ even states, we include the CSF's from the $2s^2 2p^5 3p$ and $2s 2p^6 3d$ configurations in the MCDF-AL calculations.

The $2s 2p^6 3p$ $J=1$ states are strongly perturbed by the $2s^2 2p^4 3p$ $n(\varepsilon)d$ Rydberg series. Consequently, the energies of the $3p \rightarrow 2s$ transition will be affected. These perturbations which reduce the transition energy are induced by the Coster-Kronig (or super CK) fluctuations of the core hole to intermediate levels of the CK type. An energy shift of approximately 2 eV for the $2s 2p^6 3p$ $J=1$ was obtained by performing separate MCDF calculations in the optimal level scheme, using CSF's from the $2s 2p^6 3p$ and $2s^2 2p^4 3p\, 3d$ configurations.

The residual correlation energies neglected in the present calculations come mostly from the ground-state correlation corrections[6] which arise because pairs are broken in the excitation process. The ground-state correlation corrections for transitions to a $2p$ and a $2s$ vacancy have been estimated to be 1.7 and 1.0 eV, respectively,[7] using the nonrelativistic pair energies.[8]

As an alternate approach, we also compared our experiment to theoretical calculations based on the unresolved transition array[9] (UTA) formalism. This formalism describes the totality of the transitions occurring between two electronic configurations which coalesce due to broadening effects into unresolved broad features. The energies of the transitions considered are obtained from *ab initio* atomic-structure codes, in this case the relativistic parametric potential code[10] (RELAC). Local thermodynamic equilibrium is assumed for the populations of the levels and by using the electric dipole transition probabilities and some arbitrary instrumental broadening the UTA's are calculated. In the calculation, line strengths, $|\langle a|\mathbf{D}|b\rangle|$, with $\mathbf{D}$ the electric dipole moment of the atom and $a,b$, respectively, the final and initial states, are used instead of intensities. This is equivalent to the assumption of statistical population in the initial configuration.

It is interesting to note that the UTA formalism, developed for totally different systems than ours (spark or laser produced plasmas) describes our beam-foil produced satellite lines reasonably well. The UTA's presented here[11] are derived for the Na- and Mg-like transitions in the vicinity of the Ne-like lines. The Na- and Mg-like configurations are obtained from the corresponding Ne-like ones with 1 or 2 spectator electrons added in the $n=3$ and $n=4$ shells. The Ne-like lines which serve as the starting point for the UTA calculations are also presented.

## III. EXPERIMENTAL TECHNIQUES

The experiment was performed on the UNILAC accelerator at Gesellschaft für Schwerionenforschung, Darmstadt. Figure 1 shows the experimental setup of our spectrometer on the $X2$ line of the UNILAC accelerator. The incident $Bi^{30+}$ beam at 17.3 MeV/amu passes through a 630 $\mu g/cm^2$ C stripper foil to produce charge states in the regime close to Ne-like. The charge state distribution observed after the stripper foil is shown in Fig. 2. Higher percentages of F- and Ne-like charge states were previously seen with thick (1.2 $mg/cm^2$) Be foils,[1,13] but the large uncertainties associated with the energy loss in these targets led us to use the thin carbon ones in the present experiment. The stripped beam is then charge analyzed by a magnetic dipole. Na-like ions are then selected and brought onto our exciter foil (25 $\mu g/cm^2$) where direct excitation, ionization, and single-electron capture in excited states occur. Several beam profilers are mounted in the beam line before and after the exciting foil and are checked before, after, and during a run to ensure stability of the beam alignment. A Faraday cup, mounted at the end of the beam line, serves as an absolute reference of the beam current. A Si(Li) detector, mounted on our spectrometer, views the exciter foil at an angle of 45° with respect to the beam and is used for normalizing purposes. A typical beam obtained before our spectrometer was 0.5–1 particle nA, with a spot diameter of approximately 6 mm (total beam divergence approximately equal to 1.6 mrad).

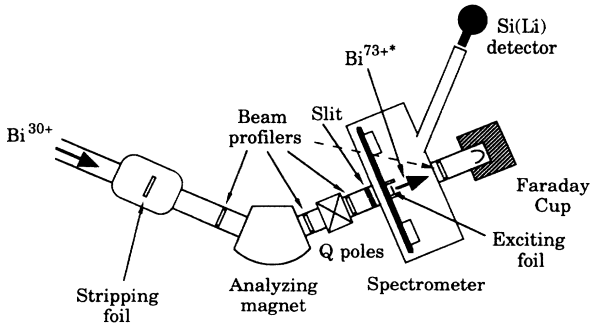


FIG. 1. Schematic of the experimental setup on the $X2$ beam line at GSI, Darmstadt.

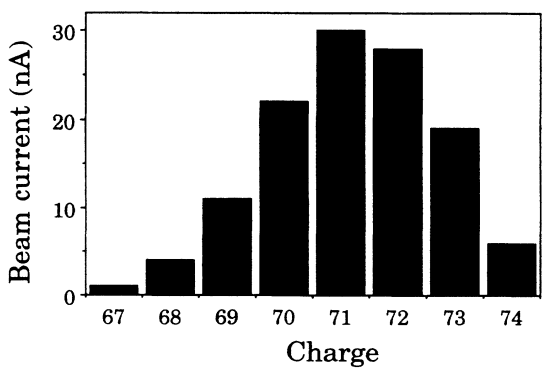


FIG. 2. Charge state distribution obtained by passing a $Bi^{30+}$ 17.3-MeV/amu beam through a 630-$\mu g/cm^2$ Be foil.

Our instrument is the Lawrence Livermore National Laboratory (LLNL) double-crystal Johann spectrometer[12] shown in Fig. 3. The spectrometer covers a 10°–18° range of Bragg angles which, with the Ge(220) crystals used in this experiment, corresponds to an energy range of 10–15 keV. As the crucial problem in fast beam-foil measurements is estimating the Doppler shifts associated with the beam velocities ($\beta \approx 0.1-0.2$), the spectrometer was designed with this very idea in mind. The twin crystals of rather large angular acceptance are irradiated by x-rays coming from the foil which is located perpendicular to the beam and in the instrumental plane of the two 1-m Rowland circles. The x-rays are detected by film (Kodak DEF 392) located on the Rowland circles.

Throughout the duration of an exposure, the position of the exciter foil is imaged through a set of two slits located in the instrument plane on two proportional counters placed on both sides of the spectrometer. By maximizing the counting rate on the proportional counters, the foil position along the beam direction is tracked with an accuracy of the order of 100–200 $\mu$m. Previously aligned thin tungsten wires of high absorption coefficient, located in front of the film holders, cast shadows onto the films. This serves to locate the position of the instrument plane (zero linear Doppler shift) on the films. A miniature x-ray tube can be remotely inserted in front of the crystals, in the position of the exciter foil. Electron beam bombardment of powdered elements (Y, $SrBr_2$, and Ge) attached to the anode using silver epoxy provides a convenient source of calibrated x rays. Short exposures (15–20 min) with this source are performed immediately before the beginning of each run to calibrate the films. The x-ray source is removed and the foil is moved into position. The x rays emitted by the target have a range of wavelengths associated with the emission angle with respect to the beam ($\theta$). Hence the beam lines will be slanted on the film with respect to the stationary calibration lines obtained from the x-ray tube. Deviations from the beam direction can be eliminated by averaging the wavelengths on the two films, red-shifted lines on one film canceling the respective blue-shifted ones on the other film. The linear Doppler shift is thus eliminated and only the second-order corrections due to the beam velocity ($\gamma$) are applied.

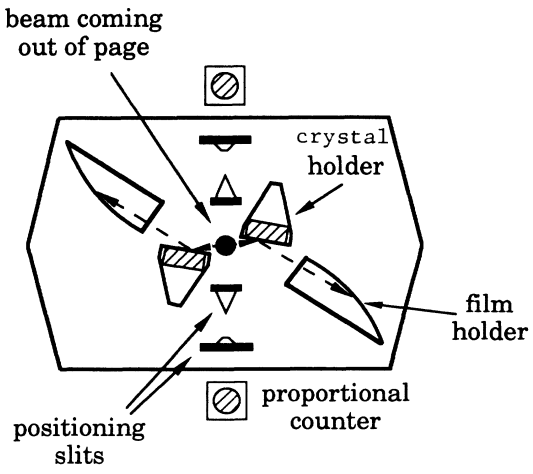


FIG. 3. Schematic of the LLNL double-crystal spectrometer.

## IV. DATA ANALYSIS AND RESULTS

A typical film exposure in the above configuration is about 8–10 h for a total accumulated charge of 2–5 mC. The films, which are coated with emulsion on one side only to avoid parallax effects, are developed and fixed. The films are then digitized by a Perkin-Elmer Micro-10 microdensitometer interfaced to a Sun 3/280 minicomputer. The films can be scanned with variable step sizes on the $x$ and $y$ axes (here $25 \times 125$ $\mu m^2$). The spectral data recorded on the film is three dimensional as can be seen in Fig. 4. The dispersion axis is horizontal, the vertical axis contains the x-ray versus beam-angle information and exhibits the Doppler shifts. The intensity of the x rays is recorded as film density. The calibration lines recorded independently at the beginning of each exposure and which are obtained from suitable $K\alpha$ fluorescence of various elements are not Doppler shifted and are thus recorded as straight lines on the film. The scan of our films yielded images of 60 rows by 7200 columns which processed as horizontal strips produce 60 spectra of 7200 channels each. By simply summing these spectra over the $y$ axis we obtain a spectrum containing the calibration lines with a very good signal-to-noise ratio. This spectrum is fitted with a least-squares deconvolution program which uses Voigt profiles obtained from the Gaussian (instrumental broadening) and Lorentzian (natural width) contributions. The beam lines which appear as slanted lines on the film have to be corrected for this effect prior to summing them up. This is done by fitting one of the intense lines on several spectra at various $y$ positions. The position of the centroid of this line is a quadratic function of the $y$ position. Using an interpolation algorithm, the spectra are shifted individually towards the base-line position as in Fig. 4. The shift is a function of $y$ as deduced from the slope of the slanted line. The spectra are then summed over the $y$ axis and the beam lines which are now straight are fitted using the deconvolution program. The final positions are obtained by shifting the lines towards the position where the Doppler shift is zero. This position is determined by analyzing the shadows that the wires cast onto the films (see Fig. 4).

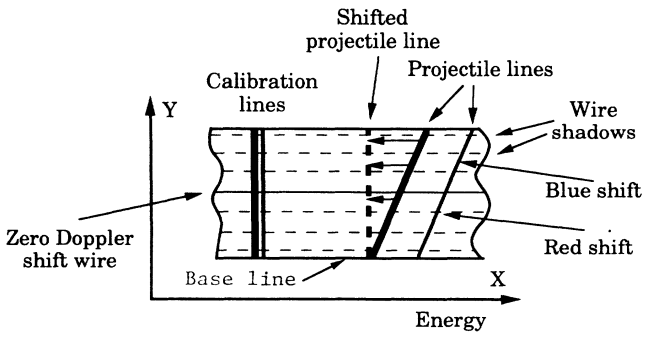


FIG. 4. Schematic of the lines recorded on film.

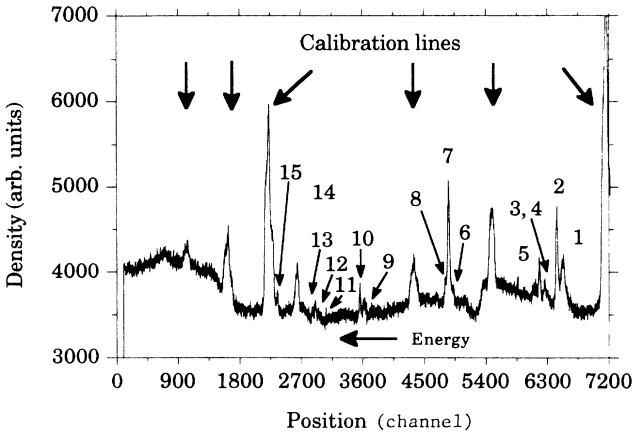


FIG. 5. Typical spectrum obtained for a 4-mC exposure. The transitions are labeled in order of increasing energy as in Table I.

We present in Fig. 5 a typical spectrum of the beam lines shifted and summed up. The calibration lines which were initially straight are slanted and broadened after the summing procedure. The beam lines are calibrated using the calibration curve deduced from the following formula:

$$\arcsin\left[\frac{\lambda}{2d}\right]=\frac{x}{R_C}+C\ .$$

Here $R_C$ and $2d$ are, respectively, the radius of curvature and the spacing of the crystals, $\lambda$ the corresponding wavelength, $C$ a constant, and $x$ the position in channels. As the radius of curvature is set through an interferometric procedure which allows precisions on the order of $10^{-4}$–$10^{-5}$, this provides a further check of the accuracy of the calibration and fitting method. An exposure is obtained simultaneously on both films and the results are averaged to obtain the final result. The energies thus obtained are corrected for the second-order Doppler effect using the $\gamma$ coefficient. The beam velocity is measured in a time-of-flight (TOF) spectrometer with a precision of approximately $2\times10^{-3}$ and further corrected for energy losses in the stripper and exciter foils. The errors are obtained by direct propagation through the correction procedures mentioned above. The main sources of error are the statistical errors in the fitting routines, the uncertainties in the determination of the $\gamma$ coefficient, and the errors in the energy calibration.

We present in Table I our results for the Ne-like lines together with the satellite Na- and Mg-like lines labeled in order of increasing energy (as in Fig. 5). The theoretical results presented in Sec. II are also shown for comparison. The MCDF-H and MCDF-S denote, respectively, calculations using hydrogenic self-energies and screened self-energies. The UTA energies were calculated as satellites associated with the Ne-like lines, using the RELAC structure code.

## V. DISCUSSION

The discussion of the results obtained will be done by comparing them to the two different theoretical calcula-

TABLE I. Bismuth Ne-, Na-, and Mg-like $n=3$ to 2 transition energies in eV. The experimental results are compared to MCDF and UTA calculations.

| Number | Upper state (hole-electron) $J$ | Experiment | UTA | Theory (MCDF-H) | (MCDF-S) |
|---|---|---|---|---|---|
| | | Ne-like | | | |
| 2 | $(2p_{3/2}\text{-}3s_{1/2})$ 1 | 10 507.82±1.21 | 10 506 | 10 507.7 | 10 507.4 |
| 5 | $(2p_{3/2}\text{-}3p_{1/2})$ 2 | 10 680.92±1.28 | 10 682 | 10 677.0 | 10 678.9 |
| 8 | $(2p_{3/2}\text{-}3d_{5/2})$ 1 | 11 722.20±1.75 | 11 729 | 11 723.5 | 11 725.9 |
| 10 | $(2p_{1/2}\text{-}3s_{1/2})$ 1 | 12 874.09±1.50 | 12 871 | 12 872.3 | 12 872.1 |
| 13 | $(2s_{1/2}\text{-}3p_{1/2})$ 1 | 13 626.73±2.34 | 13 649 | 13 627.1 | 13 633.1 |
| | | Na-like | | | |
| 1 | $(2p_{3/2}\text{-}3s_{1/2})$ 1 | 10 451.44±1.64 | 10 444 | | |
| 4 | $(2p_{3/2}\text{-}3p_{1/2})$ 2 | 10 628.86±1.56 | | | |
| 7 | $(2p_{3/2}\text{-}3d_{5/2})$ 1 | 11 682.99±1.27 | 11 674 | | |
| 9 | $(2p_{1/2}\text{-}3s_{1/2})$ 1 | 12 815.01±1.90 | 12 821 | | |
| 12 | $(2s_{1/2}\text{-}3p_{1/2})$ 1 | 13 571.84±2.40 | 13 609 | | |
| 14 | $(2p_{1/2}\text{-}3d_{3/2})$ 1 | 13 881.18±1.60 | 13 883 | | |
| 15 | $(2s_{1/2}\text{-}3p_{3/2})$ 1 | 14 232.72±1.99 | 14 250 | | |
| | | Mg-like | | | |
| 3 | $(2p_{3/2}\text{-}3p_{1/2})$ 2 | 10 600.41±2.34 | | | |
| 6 | $(2p_{3/2}\text{-}3d_{5/2})$ 1 | 11 640.63±2.95 | 11 630 | | |
| 11 | $(2s_{1/2}\text{-}3p_{1/2})$ 1 | 13 516.04±3.34 | 13 549 | | |

tions and conclusions on the applicability of each will be consequently drawn. Our experiment is a continuation of earlier work on Ne-like systems, where similar results[1,13] obtained for high-$Z$ elements (Bi,Au,Rh,La) in beam-foil experiments showed several trends exhibited by the data when compared to the MCDF calculations. Recently,[14] we reported results obtained for the same transitions on Ne-, Na, and Mg-like Au which confirm these trends with a lower degree of accuracy. A quite different type of measurement of the same transitions in lighter elements, performed on tokamaks,[7] corroborated these results with a higher degree of accuracy. Thus it seems useful to compare our Ne-like results with similar ones obtained by Beiersdorfer *et al.*[7] in order to substantiate the various trends exhibited by the data. Moreover, their theoretical results were obtained by performing the same MCDF calculations as ours.

The MCDF results are of considerably higher accuracy than the UTA calculations so they will be compared to our Ne-like results. The UTA calculations use the Ne-like lines calculated by the RELAC program as the starting point but relatively large shifts from the MCDF results are obtained. Due to the difference in population mechanisms between the beam-foil and plasma environments, agreement between experiment and theory largely within the UTA linewidths is considered quite satisfactory in our case.

### A. Ne-like results

#### *1. Comparison with the MCDF calculations*

The agreement between theory and experiment for the $2s$-$3p$ transition energy is greatly improved if one uses the hydrogenic self-energies (MCDF-H). This seems to indicate that the built-in effective-charge screening procedure tends to overestimate the screening effect in the self-energies. The same deficiency of the effective-charge screening has also been seen in the $3s$-$3p$ transitions of the Na-like ions.[15] By plotting our result together with earlier results on lighter elements[7,16] we notice that the same trend holds (see Fig. 6). One also notices that the MCDF-H calculations seem to cure this problem for all the elements shown here. However, to reach a definite conclusion, one needs to have a better handle on the correlation energies and more precise experiments for highly charged heavy ions.

For the transitions involving $2p$ holes: $(2p_{3/2}\text{-}3s_{1/2})$ $J=1$, $(2p_{1/2}\text{-}3s_{1/2})$ $J=1$, and $(2p_{3/2}\text{-}3p_{1/2})$ $J=2$, an approximately constant deviation of 1.5 eV between experiment and theory is due to the neglect of ground-state correlation corrections. This shift can readily be observed when plotting our results together with the ones for lighter elements as in Figs. 7(a)–7(c).

The discrepancy between experiment and theory for the $(2p_{3/2}\text{-}3d_{5/2})$ $J=1$ transition is partly due to the neglect of the ground-state correlation and the interaction with the $2p^5\,n(\varepsilon)d$ Rydberg series. These two effects are opposite in sign and partially cancel out each other. It is interesting to note here that the use of hydrogenic self-energy improves the agreement between theory and

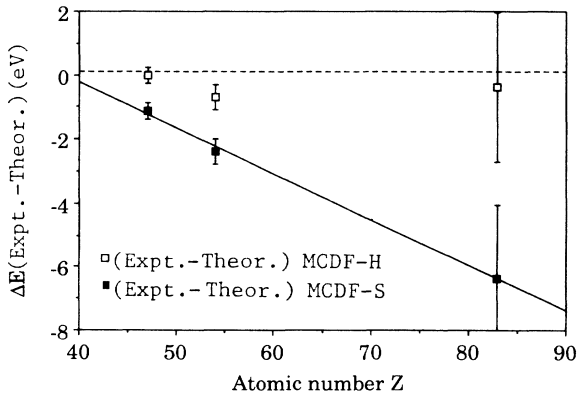


FIG. 6. Difference between theory and experiment for the $(2s_{1/2}\text{-}3p_{1/2})$ $J=1$ transition in Ne-like ions. The solid line is a linear fit to the data.

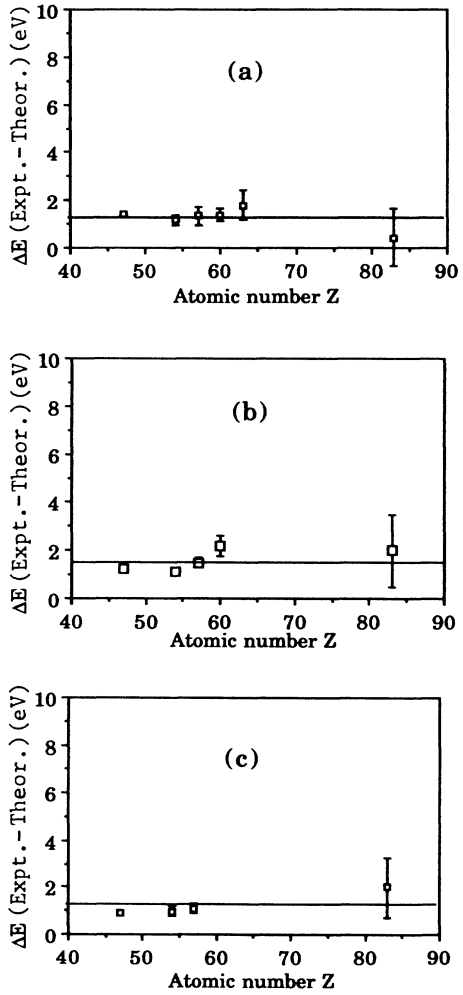


FIG. 7. Difference between MCDF-S theory and experiment for the $(2p_{3/2}\text{-}3s_{1/2})$ $J=1$ (a), $(2p_{1/2}\text{-}3s_{1/2})$ $J=1$ (b), and $(2p_{3/2}\text{-}3p_{1/2})$ $J=2$ (c) transitions in Ne-like ions. The solid lines are drawn only to guide the eye.

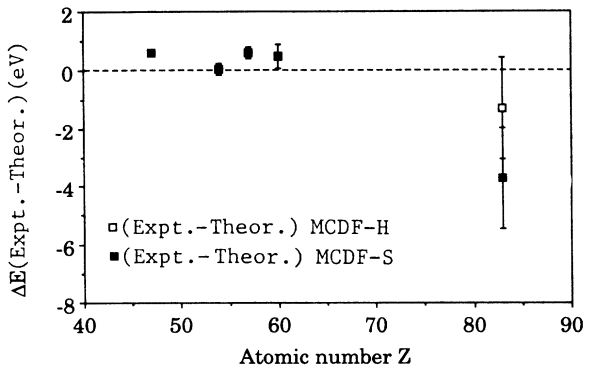


FIG. 8. Difference between MCDF theory and experiment for the $(2p_{3/2}\text{-}3d_{5/2})$ $J=1$ transition in Ne-like ions.

experiment. As can be seen from Fig. 8 this gives rise to shifts that seem to be distributed around the theoretical results.

#### 2. *Comparisons with the UTA calculations*

The UTA calculations are based on the results of the RELAC code and thus exhibit the limitations of this program. The code uses a parametric potential in a Dirac-Fock scheme and includes QED corrections. Generally speaking though, the UTA calculations do not require the knowledge of the transition energies at the level of precision attained by the MCDF codes. The goal of such calculations is to describe atomic plasmas with several ionization stages and calculate atomic parameters such as opacities or ionic temperatures. The beam foil presents a completely different system than the hot plasmas so the application of these calculations is somewhat difficult. The satellite production mechanism is here the result of single or double event processes such as capture or ionization rather than multicollisional ones. It is nevertheless useful to compare the results of such a calculation to the experiment because of its comparatively seductive simplicity and efficiency.

The Ne-like results are in good agreement with the experiment at the few eV level but their distribution around the MCDF values does not allow further inferences. In one instance the $(2s_{1/2}\text{-}3p_{1/2})$ $J=1$ transition was overestimated by about 20 eV. This difference has already been observed for lighter elements[11,14] and is partly due to the fact that the ground-state CSF's were obtained from states with filled $2s$ shells.

### B. Na- and Mg-like satellite results

This is the undisputed ground of the UTA calculations and agreement is quite satisfactory on the transitions ending on a $2p$ level (5–10 eV). As the dominant charge state in our experiment is $Bi^{72+}$, the corresponding Na-like lines will be the dominant features in the spectra. Their precision is at the 1–2-eV level and the discrepancy between theory and experiment (5–10 eV) is possibly a measure of the limitation of applicability of UTA calculations to beam-foil environments. Again in the case of the transitions ending on the $2s$ level large discrepancies were observed (25–35 eV) as a consequence of the already shifted Ne-like lines which serve as a pivot to the satellite calculations.

## VI. SUMMARY

The experimental results presented here represent a coherent set of data for the bismuth ion which is the highest Ne-like system ever studied ($Z=83$). We reported on measurements of $E1$ and $E2$ transitions in the 10–14-keV energy range for Ne-, Na-, and Mg-like ions. These were obtained by passing a Na-like beam through a very thin C foil by way of inner-shell ionization, excitation and capture processes. Theoretical results obtained with the GRASP (Refs. 3 and 4) MCDF code are presented and compared to the experimental results. UTA (Refs. 9 and 11) calculations are also presented in comparison with the experiment for the Na- and Mg-like satellites.

The comparisons with the MCDF calculations reveal differences which seem to be well understood in the framework of multielectron relativistic and correlation corrections. For transitions to a $2s$ hole state, the inclusion of energy shifts due to Coster-Kronig fluctuation and the ground-state correlation correction reduces the disagreement between theory and experiment. The residual discrepancy which increases with increasing atomic number may indicate the deficiency of the phenomenological screening procedure in calculations of many-electron self-energy corrections. For the transitions to a $2p$ vacancy state, ground-state correlation corrections not included in the calculation generate a shift of about 1.5 eV. In the case of the $(2p_{3/2}\text{-}3d_{5/2})$ $J=1$ transition additional shifts in the opposite direction are produced by interaction with the $2p^5$ $nd$ Rydberg series.

The self-energy correction plays an important role in the QED corrections. In the case of the $(2s_{1/2}\text{-}3p_{1/2})$ $J=1$ transition the use of hydrogenic self-energies improves considerably the agreement between theory and experiment.

Finally, UTA results are in overall good agreement on the Na- and Mg-like satellite lines. They are useful as they provide relatively accurate results for identifying such lines in the spectra. However, discrepancies due to the difference in population mechanism assumptions and the relative imprecision of the starting Ne-like values prevent a direct comparison with the precise experimental values.

In conclusion, we have furthered the study of many-electron highly charged heavy ions to regions never attained before. The results provide challenging problems to the theory of relativistic few-electron systems in conditions of very high field. Our theoretical results attempt to explain the discrepancies between experiment and theory at the 1–2 eV level. Further results for higher-$Z$ systems in conditions which avoid the presence of multielectron satellites are needed.

## ACKNOWLEDGMENTS

This work was performed under the auspices of the U.S. Department of Energy by the Lawrence Livermore

National Laboratory under Contract No. W-7405-ENG-48 and of the Gesellschaft für Schwerionenforschung (GSI). The authors would like to thank Dr. C. Bauche-Arnoult and co-workers for the unpublished UTA results they kindly provided on short notice. Many thanks are also due to R. Morales and D. Leneman who so diligently prepared and tested the experimental apparatus and to the GSI staff who provided optimal conditions for the experiment.

[1]D. D. Dietrich, G. A. Chandler, P. O. Egan, K. P. Ziock, P. H. Mokler, S. Reusch, and D. H. H. Hoffmann, Nucl. Instrum. Methods. **B24/25**, 301 (1987).

[2]W. R. Johnson and K. T. Cheng, in *Atomic Inner-Shell Physics,* edited by B. Crasemann (Plenum, New York, 1985).

[3]I. P. Grant, B. J. McKenzie, P. H. Norrington, D. F. Mayers, and N. C. Pyper, Comput. Phys. Commun. **21**, 207 (1980).

[4]B. J. McKenzie, I. P. Grant, and P. H. Norrington, Comput. Phys. Commun. **21**, 233 (1980).

[5]P. J. Mohr, Ann. Phys. (N.Y.) **88**, 52 (1974); Phys. Rev. Lett. **34**, 1050 (1975); Phys. Rev. A **26**, 2338 (1982).

[6]M. H. Chen, B. Crasemann, N. Mårtensson, and B. Johansson, Phys. Rev. A **31**, 5561 (1985).

[7]P. Beiersdorfer, S. von Goeler, M. Bitter, E. Hinnov, R. Bell, S. Bernabei, J. Felt, K. W. Hill, R. Hulse, J. Stevens, S. Suckewer, J. Timberlake, A. Wouters, M. H. Chen, J. H. Scofield, D. D. Dietrich, M. Gerassimenko, E. Silver, R. S. Walling, and P. L. Hagelstein, Phys. Rev. A **37**, 4153 (1988).

[8]K. Jankowski, P. Malinowski, and M. Polasik, J. Chem. Phys. **76**, 448 (1982).

[9]J. Bauche, C. Bauche-Arnoult, and M. Klapisch, Nucl. Instrum. Methods B **31**, 139 (1988).

[10]M. Klapisch, J.-L. Schwob, B. S. Fraenkel, and J. Oreg, J. Opt. Soc. Am. **67**, 148 (1977).

[11]C. Bauche-Arnoult, E. Luc-Koenig, and J.-F. Wyart (private communication).

[12]D. D. Dietrich, G. A. Chandler, R. J. Fortner, C. J. Hailey, and R. E. Stewart, Phys. Rev. Lett. **54**, 1008 (1985).

[13]G. A. Chandler, Ph.D. thesis, University of California at Davis, California, 1988 (unpublished).

[14]G. A. Chandler, M. H. Chen, D. D. Dietrich, P. O. Egan, K. P. Ziock, P. H. Mokler, S. Reusch, and D. H. Hoffmann, Phys. Rev. A **39**, 565 (1989).

[15]M. H. Chen, Nucl. Instrum. Methods B **43**, 366 (1989).

[16]P. Beiersdorfer, Ph.D. thesis, Princeton University, New Jersey, 1988 (unpublished).